COBEM 2023 27TH INTERNATIONAL CONGRESS OF MECHANICAL ENGENEERING

ABCM Brazilian Society of Mechanical Sciences and Engineering
27th ABCM International Congress of Mechanical Engineering
December 04-08, 2023, Florianópolis-SC, Brazil

COB-2023-0877
COMBUSTION AND EMISSION ANALYSIS OF A SINGLE-CYLINDER COMPRESSION IGNITION ENGINE IN A DUAL-FUEL MODE WITH HVO AND BIOGAS: A CFD APPROACH

Gustavo Vieira Frez
Túlio Augusto Zucareli de Souza
Gabriel Marques Pinto
Roberto Berlini Rodrigues da Costa
Luís Filipe de Almeida Roque
Christian Jeremi R. Coronado
Fagner Luis Goulart Dias
Mechanical Engineering Institute – Federal University of Itajubá (UNIFEI), Itájubá/MG, Brazil.
gustavofrez@gmail.com
tulio_zucareli@hotmail.com
gabrielmarquespinto@gmail.com
robertoberlini@gmail.com
filiperoque1@gmail.com
christian@unifei.edu.br
fagner@unifei.edu.br

Abstract. *A significant fraction of the Brazilian transportation matrix still relies on fossil fuels that produce harmful gases through combustion. Aiming to reduce these emissions and based on technological improvements and the potential shortage of this feedstock in the future, the use of renewable fuels has been the subject of many studies, which is particularly relevant to the national energy matrix, given its well-developed agricultural sector and large usable area. In this sense, hydrotreated vegetable oil (HVO) which is produced from vegetable oils or animal fats, is a promising option to substitute fossil diesel on internal combustion engines (ICE). Dual-fuel technology is another option to achieve the desired efficiency and control of emissions in ICE, which allows the engine to take advantage of the properties of two different fuels simultaneously in a proper operation. Most of the studies on these subjects presented in the literature are experimental. In this context, this work presents a development of a 3D computational model using ANSYS/Forte to simulate a single-cylinder 4-stroke diesel engine operating in a constant velocity in single and dual-fuel mode with HVO and HVO-biogas, respectively. In the dual-fuel mode, HVO was directly injected into the combustion chamber, and the gaseous fuel (biogas) was port-injected. Experimental data was used to validate the model. The computational results for the in-cylinder pressure curves showed a good agreement with the curves obtained by experimental tests in a Buffalo BFDE 10.0 engine. Furthermore, it was observed that the maximum values of pressure, temperature, and apparent heat release rate were reduced on the dual-fuel operation. Finally, the injection of biogas in the system resulted in a longer start of combustion and a reduction in the emissions of NOx and soot, showing that the dual-fuel operation is a good strategy to reduce the pollutant emission maintaining similar operation and efficiency conditions.*

Keywords: *diesel engine, HVO, biogas, dual-fuel, CFD analysis*

1. INTRODUCTION

Since its modern conceptualization, dating from the end of the 19th century, especially by the projects of Nikolaus August Otto and Rudolf Christian Karl Diesel, internal combustion engines (ICE) are the thermal machine most used in the world, to generate work from the burning of a fuel in a controlled system (Heywood, 2018). In general, this fuel comes from a non-renewable source, like gasoline and diesel. Heavy-duty vehicles, especially in the Brazilian transportation system, depend mainly on fossil diesel.

However, over the last few years, considering the new environmental regulations and also the needing to improve the engines' efficiency and the use of combustion energy, the substitution of fossil fuels for renewable ones and the development and implementation of new technologies have been the main subjects of many research and great attraction and discussion on the automotive market and the companies in the segment.

Considering the use of biofuels, Brazil has been a pioneer country in its use and biodiesel has played a crucial role in our country's efforts to mitigate environmental pollutants and reduce fossil fuels dependence, mainly in CI engines. In this context, in 2004 was established the National Program for Biodiesel Production (PNPB) to promote its use in the country. Subsequently, in 2008, the blending of biodiesel with diesel became mandatory starting at 2% of biodiesel and

progressively increasing over the years, reaching the current level of 12% in 2023, with a prospective elevation to 15% in 2026, as stipulated in the 16th resolution by the National Petroleum Agency – ANP (Portal gov.br, 2023).

An alternative diesel-like fuel with renewable aspects is called HVO (Hydrotreated Vegetable Oil) or green diesel. This fuel is a paraffinic hydrocarbon, with a chemical formula C_nH_{2n+2}, produced through the hydrotreating of vegetable oils, such as soybean and palm oil, or animal fats. It is already available in the European and US markets and can be used in compression ignition engines mixed with petrodiesel or as a pure fuel, given its good burning and physicochemical properties (Aatola et al., 2009). In addition, considering the Brazilian automotive market, the use of HVO can also be highlighted by the flexibility of the productive routes and adaptability of the freight transport sector, whose mobility is predominantly made by heavy vehicles, which are powered by compression ignition ICEs.

Comparing these two biofuels (HVO and biodiesel), HVO has a higher cetane number, better cold-weather properties, and lower fuel consumption. However, its production requires more complex technology, resulting in higher costs and a still limited production capacity (De Souza et al., 2022).

Considering the potential use of HVO in internal combustion engines, many studies (almost exclusively experimental ones) have been carried out to evaluate its combustion characteristics, performance, and emissions.

For example, Aatola et al. (2009) observed that the use of pure HVO in a 6-cylinder turbocharged heavy-duty diesel engine reduced the emissions of THC (total hydrocarbons), NOx, CO and smoke for all loads and engine speeds analyzed, considering the engine without change and the optimization of the injection parameters. Reductions were also observed in a blend of 30% of HVO and 70% of fossil diesel.

Comparisons between fossil diesel and HVO were also presented by Pirjola et al. (2017), considering a 4-cylinder engine and stationary and transient tests. They concluded that substituting diesel with HVO resulted in reductions in the emissions levels of nitrogen oxides and particles in both types of tests.

Bohl et al. (2018) investigated experimentally the spray and combustion characteristics of HVO and its blends with mineral diesel. It was observed that the pure HVO spray presented a shorter penetration length, a lower Sauter Mean Diameter, and a wider cone angle compared to pure mineral diesel, contributing to better air-fuel mixing. Besides, a higher percentage of HVO in the blends resulted in reductions of BSFC (brake-specific fuel consumption), particulate number, CO, and THC emissions, but not in the NOx emission levels, maintaining a similar shape to the HRR curves.

The same trend was observed by Kim et al. (2014), considering a light-duty diesel engine, that reported reductions in total HC, CO, and fuel consumption using HVO as fuel, compared to petrodiesel and FAMEs (fatty acid methyl esters).

The replacement of fossil diesel by HVO and farnesane in a single-cylinder was experimentally tested by Da Costa et al. (2022). They observed that the HVO combustions presented a shorter ID (ignition delay) and combustion duration, reducing the peaks of in-cylinder pressure and HRR (heat release rate). Moreover, the HVO combustion led to reduced NO_x, CO, CO_2, HC, and PM (particulate matter).

Another way to use renewable fuels in combustion engines is the dual-fuel (DF) technology, which consists of an engines conversion to operate with a secondary fuel, in general with low reactivity such as natural gas, biogas, and ethanol, taking some advantages from the two fuels (Karim, 2015; Da Costa et al., 2022). The simplest way of DF operation is the port-fuel injection (PFI) of the low reactivity fuel (LRF), i.e., it is admitted premixed with the intake air in the combustion chamber, as schematized in Figure 1, at the admission time.

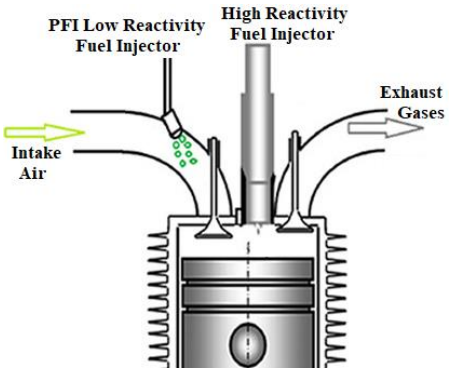

Figure 1. Schematization of dual-fuel PFI operation.

The main advantages of this technology are the reduction of fossil fuel consumption and, consequently reduction of emission levels, the improvement in the combustion control, and the cheap costs of adaptation of the base engine, at the same time as the engine performance is maintained, or improved (Karim, 2015; Da Costa et al., 2022).

In a recent study, Pinto et al. (2023) investigated the effects of fossil diesel, HVO, and farnesane in a DF operation considering a PFI injection of natural gas and biogas, It was reported that the DF operation increased the ID and decreased the combustion duration and in-cylinder pressure. Furthermore, the use of biogas reduced the emissions of NOx and PM, but increased CO, CO_2, and HC for every pilot fuel, while NG reduced NOx, PM, and CO_2, but increased CO and HC.

Analyzing the same HRF (high reactivity fuels) combustion, Da Costa et al. (2022) showed that the use of bioethanol in a DF PFI operation can reduce NOx, PM, and CO_2 emissions, in addition to the reductions of in-cylinder pressure and temperature. Lower peaks of HRR and diffusive and total combustion durations were also observed, whereas CO and HC emissions were increased in dual-fuel mode.

Another research considering HVO as pilot fuel and biogas as secondary fuel was carried out by Rimkus et al. (2020). Their results showed that the engine efficiency, peaks of in-cylinder pressure, and HRR were reduced in the DF operation followed by reductions in NOx and smoke emissions. On the other hand, the fuel consumption and the emissions of HC and CO were increased.

Despite most of the research on ICEs being limited to experimental approaches, computational ones have been also applied for improving the understanding of all processes, such as admission and exhaust flow, combustion, performance, and emissions (Merker et al., 2012; Zehni et al., 2020). Another relevant application of ICEs simulation is its use for carrying out optimization studies considering geometric design and operational parameters, such as presented by Sener et al. (2019), Ekin et al. (2022), and Liu et al. (2023).

In this sense, Merker et al. (2012) show that a computational approach can be carried out considering a 0-D (thermodynamic model), 1-D (phenomenological model), or 3D (spatial model) analysis. Considering the more detailed and complex computational analysis (3D model), the results are obtained from the solution of the mass, species, momentum, and energy conservation equations, coupled to turbulence, spray, and chemical kinetics models (Merker et al., 2012). CFD approaches considering dual-fuel combustion in CI engines are presented, for example, in the studies of Datta & Mandal (2016), Liu et al. (2022), Ekin et al. (2022), Karimi et al. (2022) and De Souza et al. (2023).

Considering the combustion of new fuels and/or blends, a proper kinetic mechanism must be used, or created. There are a few approaches to this, such as shock tube experiments or optimization of the rates of reaction to adjust the numerical results to the available experimental data. Considering the use of this methodology, recently Yu & Zhao (2020) used the Non-dominated Sorting Generic Algorithm (NSGA-II) to optimize the pre-exponential Arrhenius factor of selected reactions and produce a surrogate model for diesel and jet fuels. Another research in this sense was presented by Tay et al. (2020), which developed a highly compact and robust chemical reaction mechanism for furan oxidation in ICE, considering a GA (genetic algorithm) to optimize the pre-exponential factors in Arrhenius equations. Also, Wu et al. (2021) adjust the Arrhenius law coefficients and validate a surrogate model for furan group biofuels in internal combustion engines considering a GA.

In this sense, the present manuscript brings a CFD approach for predicting the combustion and emissions of a diesel engine, considering HVO as pilot fuel and dual-fuel combustion with HVO and biogas. Experimental tests were used to obtain the initial conditions, validate the numerical results, and also to adjust the pre-exponential factors in Arrhenius law, considering a meta-heuristic optimization algorithm, to predict the single and dual-fuel combustion of HVO, which does not have a defined kinetic mechanism in the literature. This work represents an innovative study in computational modeling of HVO combustion by CFD simulations, which are not available in the literature

2. MATERIALS AND METHODS

This study was divided into two parts: experimental and 3D-computational analysis, considering a four-stroke, single-cylinder, compression ignition engine, model Buffalo BFDE 10.0. This engine is commonly used for small-scale power generation and its main specifications are presented in Table 1. Its use is normally in a single-fuel operation, so, it was adopted to be used in a dual-fuel mode considering the port-fuel injection type for the LRF.

Table 1. Main specifications of the Buffalo BFDE 10.0 engine.

Displaced volume [cm^3]	418
Bore diameter [mm]	86
Stroke [mm]	72
Connecting rod length [mm]	118
Crank radius [mm]	38
Volumetric compression ratio	19.0:1
Maximum torque [N·m]	27
Maximum power [kW]	7.4
Number of valves	1 admission, 1 exhaust
Pilot fuel injection	Direct injection (mechanical)
Number of injector holes	4
Injection advance	22°±1° BTDC
Injection pressure [MPa]	19.6

2.1 Experimental setup

The experimental part was carried out at the Thermal Machines Laboratory (LMT), at Federal University of Itajubá (UNIFEI), Brazil.

Similar to the schematization in Figure 1, the experimental tests considered the direct injection of the high-reactivity fuel (HVO) in the combustion chamber at constant pressure and injection advance through a 4-holed injector, as shown in Table 1. The low-reactivity fuel (biogas) was port-fuel injected (PFI) with a 3 holes Bosch PFI injector near the intake valve. The consumption of the fuels used in the tests was obtained considering the measurements with a volumetric sensor and a mass flow meter for pilot fuel and biogas, respectively (Da Costa et al., 2022).

The engine velocity and the Indicated Mean Effective Pressure (IMEP) were kept constant during the experimental tests, respectively 1800 rpm and 5 bar, using a hydraulic dynamometer to control the engine load. A piezoelectric transducer and an optical encoder were used to measure the in-cylinder pressure and the crank angle values for each cycle, while the air-fuel ratio was measured by a Bosch lambda sensor. Besides, an air box, an air filter, a restriction valve, and a flow meter equipped with temperature, pressure, and humidity sensors were used at the intake system. The details of the measuring instruments can be found in Da Costa et al. (2022). Finally, other parameters were kept constant in order to ensure that all tested scenarios had comparable conditions. The engine test bench is schematized in Figure 2.

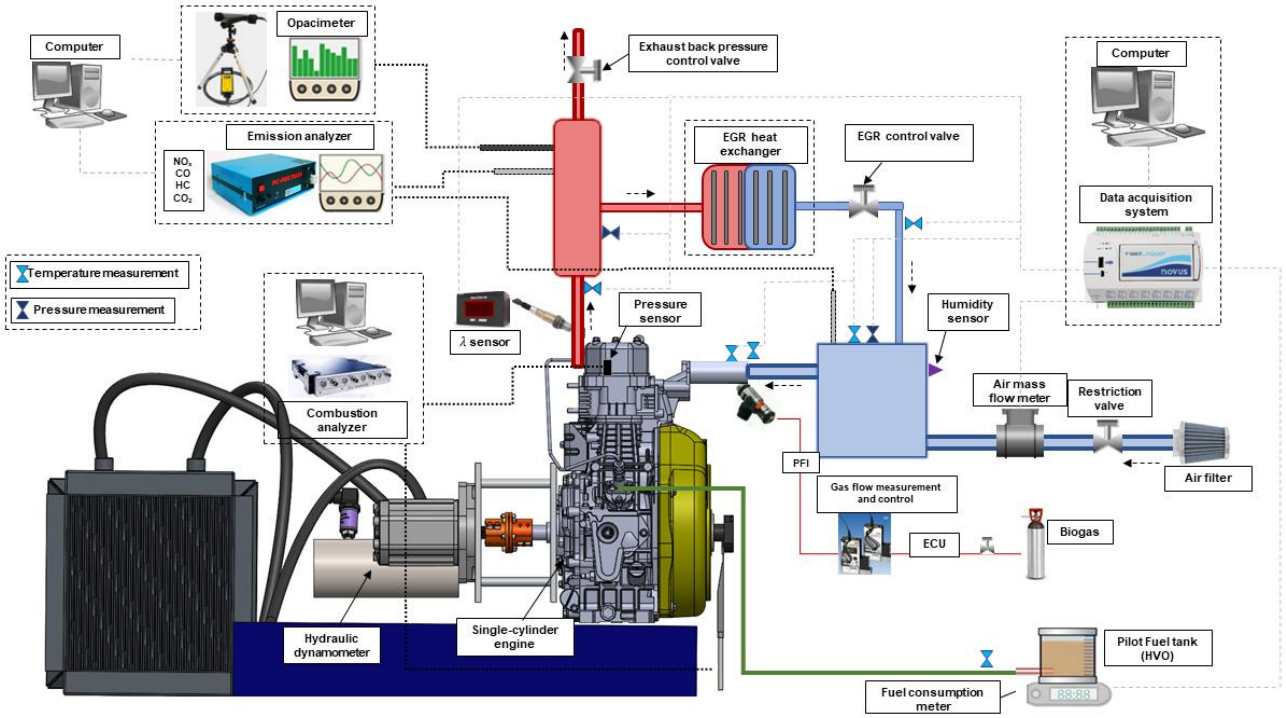

Figure 2. Schematic diagram of the experimental engine test bench, considering the dual-fuel operation.

The HVO, used as the pilot fuel, was imported from NESTE Corporation, while the biogas considered in the experiments was synthetically manufactured. Table 2 presents the main physicochemical properties of these fuels.

Table 2. Main physicochemical properties of HVO and biogas.

Property	**HVO** (Da Costa et al., 2022)
Molecular formula	$C_{14}H_{30}$
H/C ratio	2.14
$AFR_{stoichiometric}$	14.97
LHV [MJ/kg]	44.10
Cetane number	76.3
Density at 20 °C [kg/m^3]	780.0
Viscosity at 40 °C [mm^2/s]	2.82

Property	**Biogas** (Pinto et al., 2023)
Composition	CH_4 = 64.7%; CO_2 = 34.3%
H/C ratio	4
$AFR_{stoichiometric}$	6.94
LHV [MJ/kg]	20.19
Octane number	130
$T_{autoignition}$ [°C]	650
$T_{adiabatic\ flame}$ [°C]	~1872−1926

2.2 Computational modeling

The computational part of this research was also carried out at Thermal Machines Laboratory (LMT), considering the ANSYS® platform version 2022 R1.

A CAD model of the engine combustion chamber was developed in SpaceClaim, based on a sector of 90°, which is proportional to the number of holes of the injector, as shown in Table 1, aiming to decrease the computational time of the simulations. Figure 3 shows the combustion chamber designed at the bottom dead center (a) with its temperature boundary conditions, and the pilot fuel spray representation at the x-z plane (b), where α is the cone angle, and its mesh (c) with 134,936 elements, both at the top dead center. This mesh was chosen, considering a mesh independence study performed by Frez (2022).

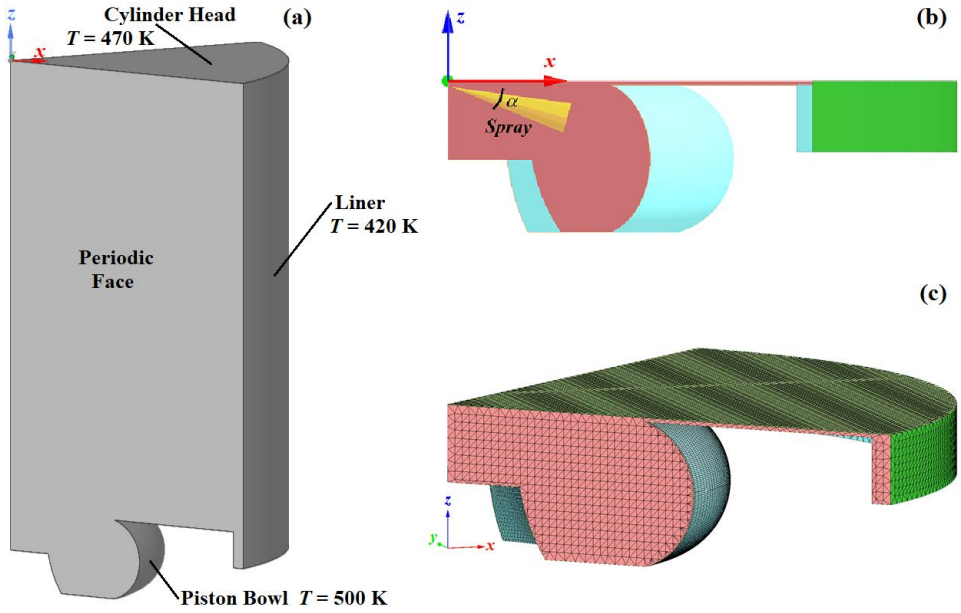

Figure 3. Spatial representation of the combustion chamber used in CFD analysis.

The 3D combustion process was performed using Forte software, considering the crank-angle interval between the IVC (Inlet Valve Closing) and the EVO (Exhaust Valve Opening) points, which were obtained from the experiments. Forte is an ANSYS software dedicated to 3D computational simulation of internal combustion engines, solving the equations of conservation of mass, species, momentum, and energy, described by Eqs. (1)-(4), coupled to turbulence, and spray models and also chemical kinetics (ANSYS, 2022), modeled by the modified Arrhenius law, Eq. (5).

$$\frac{\partial \rho}{\partial t} + \nabla \cdot (\rho \boldsymbol{u}) = \dot{\rho}^S \tag{1}$$

where ρ is the density, $\boldsymbol{u}$ is the flow velocity vector and $\dot{\rho}^S$ is the source term due to spray evaporation.

$$\frac{\partial \rho_i}{\partial t} + \nabla \cdot (\rho_i \boldsymbol{u}) = \nabla \cdot [\rho D (\nabla y_i)] + \nabla \cdot \boldsymbol{\phi} + \dot{\rho}_\iota{}^C + \dot{\rho}_\iota{}^S \quad \text{with } i = 1,2,\dots,N \tag{2}$$

where the subscript i is the species index, N is the total number of species, D is the molecular diffusion coefficient, $y_i = \rho_i/\rho$ is the mass fraction, $\boldsymbol{\phi}$ is the term that accounts the effects of the convection term and $\dot{\rho}_\iota{}^C$ is the source term due to chemical reactions.

$$\frac{\partial \rho \boldsymbol{u}}{\partial t} + \nabla \cdot (\rho \boldsymbol{u}\boldsymbol{u}) = -\nabla p + \nabla \cdot \boldsymbol{\sigma} - \nabla \cdot \boldsymbol{\Gamma} + \rho \boldsymbol{g} + \boldsymbol{F}^S \tag{3}$$

where p is the pressure, $\boldsymbol{\sigma}$ is the viscous shear stress tensor, $\boldsymbol{\Gamma}$ is the stress tensor that accounts the effects of the nonlinear convection term, $\boldsymbol{g}$ is the gravity acceleration vector and $\boldsymbol{F}^S$ is the rate of momentum gain per unit of volume.

$$\frac{\partial \rho U}{\partial t} + \nabla \cdot (\rho \boldsymbol{u} U) = -p \nabla \cdot \boldsymbol{u} - \nabla \cdot \boldsymbol{J} - \nabla \cdot \boldsymbol{H} + \rho \varepsilon + \dot{Q}^C + \dot{Q}^S - \dot{Q}_{rad} \tag{4}$$

where U is the specific internal energy, $\boldsymbol{J}$ is the heat flux vector accounting for contributions due to heat conduction and enthalpy diffusion, $\boldsymbol{H}$ is the term accounting for the effects of the nonlinear convection term, ε is the dissipation rate of

the turbulent kinetic energy, $\dot{Q}^C$ and $\dot{Q}^S$ are the source terms due to chemical heat release and spray interactions, respectively and $\dot{Q}_{rad}$ is the radiative heat loss.

As suggested by Han & Reitz (1995), the turbulence was described considering the RANS RNG k-ε model, with its default constants values in Forte.

A reduced chemical kinetic model for n-heptane, composed of 29 species and 52 reactions (Patel et al., 2004), was used as the basis to obtain the kinetic model of the single and dual-fuel combustion processes considering the methodology proposed by Rahimi et al. (2010). For that, a metaheuristic optimization using Lichtenberg Algorithm (De Souza et al., 2022) was applied to a 0-D Chemkin-PRO model in order to change the pre-exponential factor of the Arrhenius law, Eq. (5), on the basis kinetic model, as performed in Yu & Zhao (2020) and Wu et al. (2021), with the ultimate goal of reducing the peak of pressure and R^2 errors between experimental data and computational ones. After that, the n-tetradecane (n-$C_{14}H_{30}$) physicochemical properties were considered to represent the high-reactivity fuel on Forte.

$$k(T) = A \cdot T^B \cdot \exp\left(-\frac{E}{RT}\right) \tag{5}$$

where k is the kinetic constant, A and B are the pre-exponential and temperature factors, respectively, and E is the activation of energy.

A solid cone injector and an adaptative collision mesh were used to model the pilot fuel spray, considering 3500 parcels, a square velocity profile of injection, and a temperature of 368 K. The injection begins at the crank angle of the static start of injection and its duration is equal to 19.5°. The total mass of both pilot and port-injected fuels was obtained from the experimental tests, considering one cycle of the engine operation. The primary and secondary spray breakups were modeled using the Kelvin-Helmholtz and Rayleigh-Taylor hybrid models (Reitz & Beale, 1999). The Han-Reitz model was considered to model the heat transfer and the wall temperatures were set to 420 K for the liner, 470 K for the head, and 500 K for the piston (ANSYS, 2022).

The starting mixture for the single-fuel operation contains only air (21% O_2 and 79% N_2, volume basis). For the dual-fuel operation, the starting mixture contains air and biogas, which volume basis was calculated considering its composition (methane and carbon dioxide) and injected mass, normalized with the air composition. Initial pressure and temperature were obtained experimentally, as the air flow masses. The velocity initialization was made considering the swirl movement with a 1.2 initial value, normal to the piston boundary. Besides, a value of 1.3 was considered as the time step growth factor, which was restricted by a maximum value of 0.5 CAD movement for each time iteration.

3. RESULTS AND DISCUSSION

This section presents the results of this study. Table 3 presents the experimental data used in the simulation studies.

Table 3. Inputs data used in the simulations obtained from the experimental tests.

Data	Fuel	
	Pure HVO	**HVO-Biogas**
p_0 [bar]	1.196	1.213
T_0 [K]	385.896	380.530
$\dot{m}_{air}$ [kg/h]	19.963	20.378
$\dot{m}_{pf}$ [kg/h]	0.6676	0.6448
$\dot{m}_{sf}$ [kg/h]	0.000	0.200
x_{O_2}	0.21*	0.207721*
x_{N_2}	0.79*	0.781427*
x_{CH_4}	-----	0.007054*
x_{CO_2}	-----	0.003798*

The subscripts pf and sf in Table 3 mean pilot fuel (HVO) and secondary fuel (biogas). *calculated. The injected mass of biogas considered in this study represents a 12.43% of energy substitution ratio (ESR).

3.1 Kinetic Model Adaptation

Similar to Rahimi et al. (2010), was considered a range of ±15% of the original pre-exponential factor values A was considered to the random population used in the optimization of the kinetic model. Avoiding high computational cost, it

was select the 8 reactions that most affect the heat release were selected, considering the pilot fuel specie (n-C_7H_{16}). For dual-fuel, it was added 1 more reaction, to consider the specie CH_4. Table 4 presents the results of the original and optimized values of *A*.

The results obtained in Table 4 represent the best results of the optimization processes, where was considered the goals: best R^2 adjust and minimum differences of the in-cylinder pressure peak (p_{max}) and the crank angle of the start of combustion (SOC) compared to experimental results.

Table 4. Original and optimized values of *A* for HVO and HVO-biogas combustion.

Reaction	Original	Optimized	
		Pure HVO	HVO-Biogas
NC7H16 + OH = C7H15-2 + H2O	$9{,}700 \cdot 10^{9}$	$8.4625 \cdot 10^{9}$	$9{,}6979 \cdot 10^{9}$
CO + OH = CO2 + H	$8{,}990 \cdot 10^{7}$	$7.6415 \cdot 10^{7}$	$8{,}0742 \cdot 10^{7}$
O + OH = O2 + H	$4{,}000 \cdot 10^{14}$	$3{,}4000 \cdot 10^{14}$	$4{,}0361 \cdot 10^{14}$
OH + OH = O + H2O	$6{,}000 \cdot 10^{8}$	$6{,}3964 \cdot 10^{8}$	$6{,}6651 \cdot 10^{8}$
H + O2 + M = HO2 + M	$3{,}600 \cdot 10^{17}$	$3{,}1708 \cdot 10^{17}$	$3{,}8439 \cdot 10^{17}$
CH2O + OH = HCO + H2O	$5{,}563 \cdot 10^{10}$	$5{,}3893 \cdot 10^{10}$	$5{,}52750 \cdot 10^{10}$
C2H4 + OH = CH2O + CH3	$6{,}000 \cdot 10^{13}$	$5{,}2506 \cdot 10^{13}$	$5{,}1006 \cdot 10^{13}$
C2H4 + OH = C2H3 + H2O	$8{,}020 \cdot 10^{13}$	$7{,}7782 \cdot 10^{13}$	$6{,}8170 \cdot 10^{13}$
CH4 + OH = CH3 + H2O	$1{,}600 \cdot 10^{6}$	-------	$1{,}8147 \cdot 10^{6}$

Figure 4 compares the curves of in-cylinder pressure obtained experimentally and computationally (with the optimized *A* values in the kinetic model, showed in Table 4). The results of R^2 and the percentual difference between experimental and computational results, for p_{max} and SOC are presented in Table 5. The SOC was estimated considering the minimum value of the pressure rise rate (PRR) curve after the start of the main fuel injection, as presented in Xin (2013).

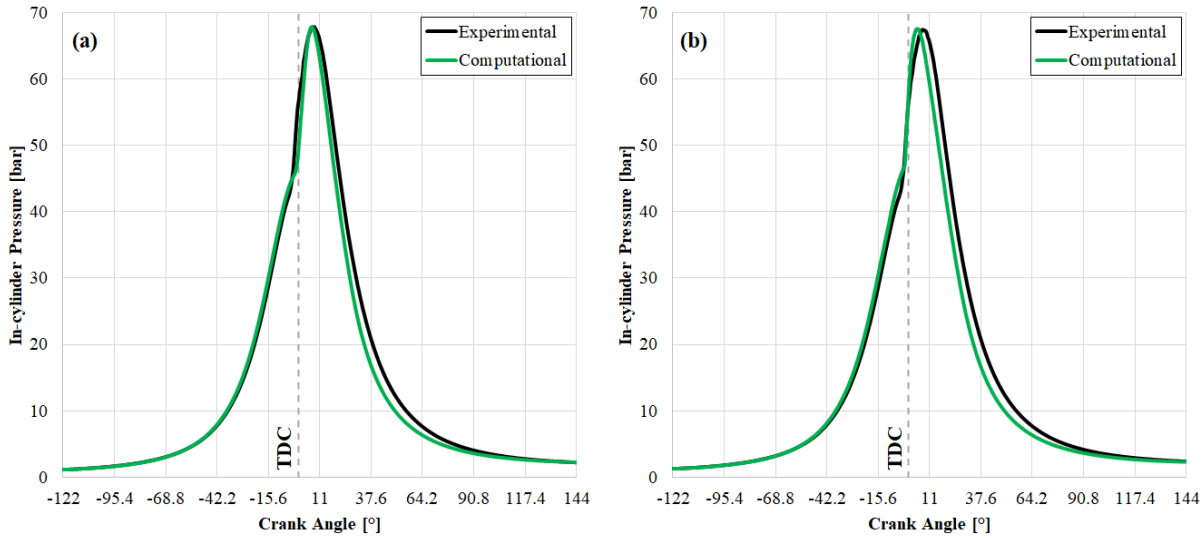

Figure 4. Comparison of in-cylinder pressure for pure HVO (a) and dual-fuel HVO-Biogas (b).

From Figure 4 and Table 5, it can be seen that the in-cylinder pressure obtained from computational results, considering the optimized *A* from the 0-D model, presented a good agreement with the experimental ones. Besides, the absolute percentual errors for the peak of pressure and SOC were below 7%. The dual-fuel combustion presented a longer delay SOC while the single-fuel presented a shorter one.

Table 5. Results for p_{max}, R^2, and the errors for the optimization process.

Fuel	R^2 [--]	Δp_{max} [%]	ΔSOC [%]
Pure HVO	0.985256	0.0475	-0.0491
HVO-Biogas	0.986389	0.0697	0.0235

3.2 CFD Analysis

After the kinetic-models optimization processes, the CFD analyses were carried out in Forte. Figure 5 presents the comparisons between single and dual-fuel combustion for AHRR curves, highlighting the SOC (-2.9° and -2.4° BTCD single-fuel and dual-fuel modes, respectively). It can be observed that the addition of biogas in the engine process caused a reduction of the AHHR peak and delayed the SOC, due to the reduction of the main-fuel injection and the presence of biogas, which contains CO_2 in its composition, in the combustion chamber that replaced the oxygen, corroborating for a delaying formation of a flammable mixture. Rimkus et al. (2020) considering a 1-D analysis also observed reductions in the AHRR peaks and the start of combustion for SF and DF operation between -3 and -2 CAD when HVO was substituted by biogas. Besides, Pinto et al. (2023) observed a delay in the SOC considering the DF combustion of HVO and biogas.

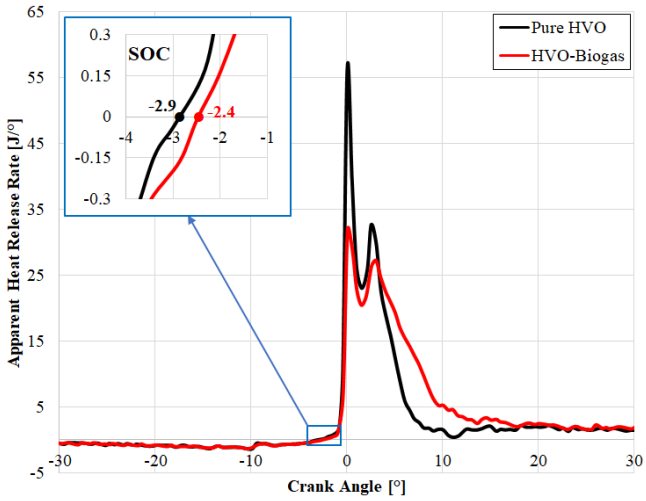

Figure 5. Comparisons of AHRR for single and dual-fuel combustion.

CFD results also showed a decrease of 2.11% in the peak of in-cylinder pressure but an increase of 3.48 to 3.96 bar in the indicated mean effective pressure for dual-fuel operation, a decrease of about 4% in the indicated specific fuel consumption and a slight reduction in the combustion efficiency, reaching 77.9% for SF and 77.5% for DF combustion. On the other hand, the maximum pressure rise rate value was reduced by 43.4% for DF combustion, following the behavior observed in the maximum value of AHRR.

Figure 6 presents the temperature fields for some crank angles. It can be seen that the temperature distribution is very similar for SF and DF operations at the same CAD, but at CAD = 0° a slight difference in the red regions indicates the delay of SOC in the DF case.

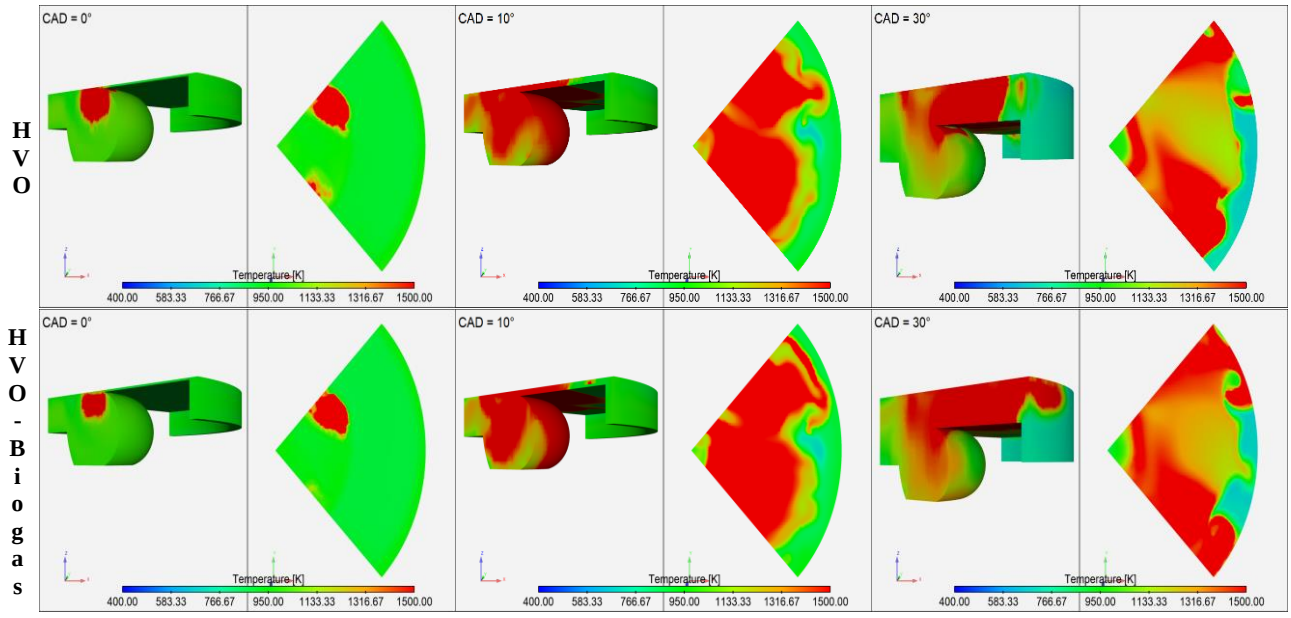

Figure 6. Temperature fields in different crank angles.

The temperature fields after TDC presents more regions with high temperatures because of the progression in the combustion process which turns more homogeneous because of the movement of the gaseous combustion in the combustion chamber. Besides, the slight difference between CAD = 10° and 30° indicates that the diffusive phase of combustion is a little longer for DF mode.

Figure 7 compares de emissions levels of soot, NOx, CO, UHC, and CO_2 for single-fuel (SF) and dual-fuel (DF) obtained from Forte simulations at exhaust valve opening (EVO) i.e., CAD = 144°.

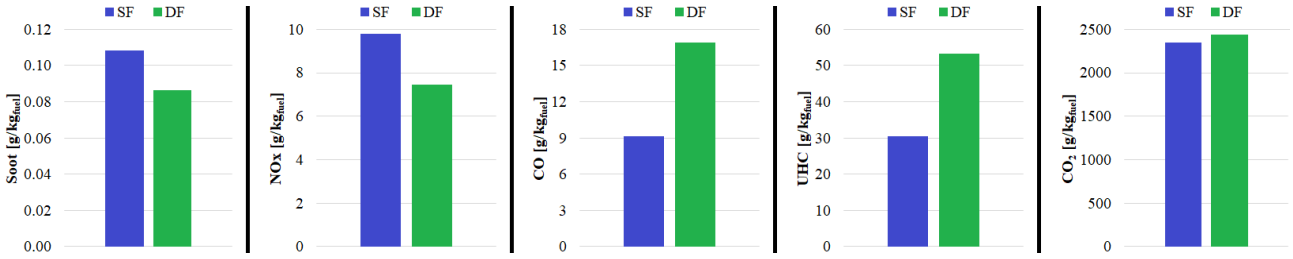

Figure 7. Emissions at EVO, for single and dual-fuel combustion.

The dual-fuel combustion decreased both soot and NOx emissions. The soot formation in DF operation decreased because of the reduction in HRF injection, which reduces the fuel-rich zones at elevated temperatures and consequently the soot formation. The presence of CO_2 in biogas composition contributes to the reduction of the in-cylinder pressure and temperature, because of the higher specific heat capacity of CO_2, that replaced part of O_2 in the combustion chamber in DF operation, which explains the increase of CO_2 emissions and also the reduction of soot in DF mode. Therefore, because of this temperature reduction contributed to the thermal NOx formation and, consequently, the levels of NOx emission. Furthermore, the increase in UHC emissions can be explained because the reduction of O_2 in the combustion chamber, replaced by biogas, contributes to the worst combustion, which causes higher incomplete combustion and, consequently, an increase in CO emissions. In addition, the reduction in the maximum in-cylinder temperature further accentuates these emissions. Similar emissions trends were observed by Rimkus et al. (2020) and Pinto et al. (2023).

4. CONCLUSIONS

The present study carried out a computational analysis of the combustion cycle of a single-cylinder CI engine operating on single and dual-fuel mode with HVO and HVO-biogas, respectively. A CFD simulation was developed based on experimental, initial, and boundary conditions by coupling transport, chemical kinetics, obtained from a 0-D model which considered a metaheuristic optimization process of the pre-exponential factor in the modified Arrhenius law, and spray models using ANSYS Forte software. The results obtained in the validation step of the kinetic model adaptation showed a good agreement between in-cylinder pressure measured experimentally and obtained computationally, achieving R^2 higher than 98.5%, peak pressure absolute error lower than 7%, and start of combustion absolute error lower than 5% for SF and DF operation. Regarding the combustion analysis, the CFD analysis was able to capture the late SOC and smaller peaks of in-cylinder pressure, PRR, AHRR, and temperature for DF operation, which were thoroughly compared with experimental data presented by previously published studies. The temperature fields presented similar distribution with slight differences, which can be explained because of the low of the LRF injected, suggesting an analysis with higher ESR. CFD results indicated that the PFI injection of biogas reduced NOx emissions by about 23.8% and soot by about 20.1% but increased UHC, CO, and CO_2 emissions because of the reduction of O_2 presence in the combustion chamber which contributed to incomplete and worse combustion. These trends of emissions are in agreement with results reported in experimental studies from the literature, further corroborating the validity of the numerical model. Finally, the verified similar combustion properties of DF and SF combustions, and also with the use of renewable diesel instead of fossil diesel, and lower emissions of regulated pollutants indicates that the use of this operation may contribute to reducing air pollution, maintaining similar conditions of operation and efficiency while using renewable and sources of energy.

5. ACKNOWLEDGEMENTS

The authors would like to acknowledge the aid and financial support provided by Fundação de Desenvolvimento da Pesquisa – Fundep Rota 2030/Linha V (Procs. 27192*5 and 27192*62) and Thermal Machines Laboratory (LMT – UNIFEI). The authors also would like to acknowledge FPT Industrial Brasil (R&D partner) and NESTE (HVO producer) for supporting the development of this research.

6. REFERENCES

Aatola, H., Larmi, M., Sarjovaara, T. and Mikkonen, S., 2009. "Hydrotreated vegetable oil (HVO) as a renewable diesel fuel: Trade-off between NOx, particulate emission, and fuel consumption of a heavy-duty engine". *SAE International Journal Engines*, Vol. 1 (1), p. 1251-1262.

ANSYS, Inc., 2022. "Forte Theory Manual – Release 2022 R1". USA.

Bohl, T., Smallbone, A., Tian, G. and Roskilly, A.P., 2018. "Particulate number and NOx trade-off comparisons between HVO and mineral diesel in HD applications". *Fuel*, Vol. 215, p. 90-101.

Da Costa, R.B.R., Roque, L.F.A., De Souza, T.A.Z., Coronado, C.J.R., Pinto, G.M., Cintra, A.J.A., Raats, O.O., Oliveira, B.M., Frez, G.V. and Da Silva M.H., 2022. "Experimental assessment of renewable diesel fuels (HVO/Farnesane) and bioethanol on dual-fuel mode". *Energy Conversion and Management*, Vol. 258, p. 115554.

Datta, A. and Mandal, B.K., 2016. "Impact of alcohol addition to diesel on the performance combustion and emissions of a compression ignition engine". *Applied Thermal Engineering*, Vol. 98, p. 670-82.

De Souza, T.A.Z., Frez, G.V., Pinto, G., Costa, R., Roque, L.F.A., Coronado, C.J.R and Vidigal, L.P.V., 2023. "CFD Analysis of Different Biogas Upgrading Levels for Dual-Fuel Operation in Diesel Engines". *SAE Technical Paper*, N. 2023-24-0055.

De Souza, T.A.Z., Pereira, J.L.J., Francisco, M.B., Sotomonte, C.A.R., Ma, B.J., Gomes, G.F. and Coronado, C.J.R., 2022. "Multi-objective optimization for methane, glycerol, and ethanol steam reforming using Lichtenberg algorithm". *International Journal of Green Energy*, Vol. 20, p. 390-407.

De Souza, T.A.Z., Pinto, G.M., Julio, A.A.V., Coronado, C.J.R., Perez-Herrera, R., Siqueira, B.O.P.S., da Costa, R.B.R., Roberts, J.J. and Palacio, J.C.E., 2022. "Biodiesel in South American countries: A review on policies, stages of development and imminent competition with hydrotreated vegetable oil". *Renewable and Sustainable Energy Reviews*, Vol. 153, 111755.

Ekin, F., Ozsoysal, O.A., and Arslan, H., 2022. "The effect of using hydrogen at partial load in a diesel-natural gas dual fuel engine". *International Journal of Hydrogen Energy*, Vol. 47(42), p. 18532-18550.

Frez, G.V., 2022. Simulação fluidodinâmica em ANSYS – CFD da combustão dual-fuel em motores de ignição por compressão utilizando diesel renovável (HVO) com biogás. M.Sc. dissertation, Graduate Program in Mechanical Engineering, Federal University of Itajubá, Itajubá, Brasil.

Han, Z., and Reitz, R. D., 1995. "Turbulence Modeling of Internal Combustion Engines Using RNG k-ε Models". *Combustion Science and Technology*, Vol. 106, p. 267-295.

Heywood, J. B., 2018. *Internal combustion engines fundamentals*. 2nd ed. New York: McGraw-Hill Education.

Karim, G. A., 2015. *Dual-fuel diesel engines*. Boca Raton: CRC Press.

Karimi, M., Wang, X., Hamilton, J. and Negnevitsky, M., 2022. "Numerical investigation on hydrogen-diesel dual-fuel engine improvements by oxygen enrichment". *International Journal of Hydrogen Energy*, Vol. 47 (60), p. 25418-25432.

Kim, D., Kim, S., Oh, S. and No, S.Y., 2014. "Engine performance and emission characteristics of hydrotreated vegetable oil in light duty diesel engines". *Fuel*, Vol. 125, p. 36-43.

Liu, J., Liu, Z., Wang, L., Wang, P., Sun, P., Ma, H. and Wu, P., 2022. "Numerical simulation and experimental investigation on pollutant emissions characteristics of PODE/methanol dual-fuel combustion". *Fuel Processing Technology*, Vol. 231, p. 107228.

Liu, X., Silva, M., Mohan, B., Al-Ramadan, A.S., Cenker, E. and Im, H.G., 2023. "Computational optimization of the performance of a heavy-duty natural gas pre-chamber engine". *Fuel*, Vol. 352, p. 129075.

Merker, G., Schwarz, C. and Teichmann, R., 2012. *Combustion Engines Development: Mixture Formation, Combustion, Emissions and Simulation*. Berlin: Springer.

Patel, A., Kong, S. and Reitz, R.D., 2004. "Development and Validation of a Reduced Reaction Mechanism for HCCI Engine Simulations". *SAE Technical Paper*, N. 2004-01-0558.

Pinto, G. M. et al., Da Costa, R.B.R., De Souza, T.A.Z., Rosa, A.J.A.C., Raats, O.O., Roque, L.F.A., Frez, G.V. and Coronado, C.J.R., 2023. "Experimental investigation of performance and emissions of a CI engine operating with HVO and farnesane in dual-fuel mode with natural gas and biogas". *Energy*, Vol. 277, p. 127648.

Pirjola, L., Rönkkö, T., Saukko, E., Parviainen, H., Malinen, V., Alanen, J. and Saveljeff, H., 2017. "Exhaust emissions of non-road mobile machine: Real-world and laboratory studies with diesel and HVO fuels". *Fuel*, Vol. 202, p. 154-164.

Portal gov.br, 2023. Governo oficializa ampliação da mistura de biodiesel no diesel vendido no país. Government Portal, https://www.gov.br/pt-br/noticias/energia-minerais-e-combustiveis/2023/03/governo-oficializa-ampliacao-da-mistura-de-biodiesel-no-diesel-vendido-no-pais. Accessed 10 October 2023.

Rahimi, A., Fatehifar, E. and Saray, R.K., 2010. "Development of an optimized chemical kinetic mechanism for homogeneous charge compression ignition combustion of a fuel blend of n-heptane and natural gas using a genetic algorithm". In *Proceedings of the Institution of Mechanical Engineers, Part D: Journal of Automobile Engineering*, Vol. 224 (9), p. 1141-1159.

Reitz, R.D. and Beale, J.C., 1999. "Modeling spray atomization with the Kelvin-Helmholtz/Rayleigh-Taylor hybrid model". *Atomization and Sprays*, Vol. 9, p. 623-650.

Rimkus, A., Stravinskas, S. and Matijošius, J., 2020. "Comparative Study on the Energetic and Ecologic Parameters of Dual Fuels (Diesel–NG and HVO–Biogas) and Conventional Diesel Fuel in a CI Engine". *Applied Sciences*, Vol. 10, p. 359.

Sener, R., Özdemir, M.R. and Yangaz, M.U., 2019. "Influence of piston bowl geometry on combustion and emission characteristics". *Journal of power and energy*, Vol. 233(5), p. 576-587.

Tay, K.L., Yang, W., Zhao, F., Lin, Q. and Wu, S., 2020. "Development of a Highly Compact and Robust Chemical Reaction Mechanism for Unsaturated Furan Oxidation in Internal Combustion Engines via a Multiobjective Genetic Algorithm and Generalized Polynomial Chaos". *Energy & fuels*, Vol. 36, p. 936-948.

Wu, S., Tay, K.L., Li, J., Yang, W. and Yang, S., 2021. "Development of a compact and robust kinetic mechanism for furan group biofuels combustion in internal combustion engines". *Fuel*, Vol. 298, p. 120824.

Xin, Q. Fundamentals of dynamic and static diesel engine system designs. Chapter 4. Book: Diesel Engine System Design. Woodhead Publishing: 2013, p. 299-347.

Yu, W. and Zhao, F., 2020. "Formulating of model-based surrogates of jet fuel and diesel fuel by an intelligent methodology with uncertainties analysis". *Fuel*, Vol. 268, p. 117393.

Zehni, A., Balazadeh, N., Hajibabaei, M. and Poorghasemi, K., 2020. "Numerical study of the effects of split injection strategy and swirl ratio for biodiesel PCCI combustion and emissions". *Propulsion and Power Research*, Vol. 9(4), p. 355-371.

7. RESPONSIBILITY NOTICE

The authors are the only ones responsible for the printed material included in this paper.